PCCP

Accepted Manuscript

ROYAL SOCIETY OF CHEMISTRY

www.rsc.org/pccp

Journal Name

ARTICLE

Effects of Pt Dispersion on Electronic and Oxide Ionic Conductivity in $Pr_{1.90}Ni_{0.71}Cu_{0.24}Ga_{0.05}O_4$

Received 00th January 20xx,
Accepted 00th January 20xx

DOI: 10.1039/x0xx00000x

www.rsc.org/

T. Ishihara [a,b] J. Hyodo [a], H. Schraknepper [a], K. Tominaga [a], S. Ida [a,b],

The effects of dispersing Pt particles in bulk $Pr_{1.90}Ni_{0.71}Cu_{0.21}Ga_{0.05}O_{4+\delta}$ (PNCG) on the electrical conductivity and oxygen permeability of the material were studied. The different thermal expansion coefficients of PNCG and Pt generated a mechanical compressive strain in the PNCG. This may cause the electrical conductivity decreased in samples containing Pt. In contrast, oxide ion conductivity estimated from oxygen permeability was increased by dispersion of Pt. These variations appear to be related to the electron hole and interstitial oxygen concentrations. Moreover, the present study suggests that the mechanical strain induces a chemical strain via the introduction of oxygen defects as well as changes in cation valences.

Introduction

The residual lattice strain in oxide ion conductors such as ZrO_2 or CeO_2 has been recently attracting significant interest due to reports that this effect can increase the oxide ion conductivity in conventional materials by several orders of magnitude. The majority of studies concerning residual strain effects have been performed using epitaxial grown thin films.[1–5] The strain in such films originates from the mismatch between the lattice constants of the substrate and the film. Thus, in the case of epitaxial thin films, the strain at the interface between the substrate and the thin film can be controlled by varying the relationship between the lattice constants as well as the thermal expansion coefficients and temperatures of the substrate and film. However, variations in thin film strains are difficult to observe macroscopically. Thus, in order to examine the effects of lattice strain, it is necessary to induce a similar strain in the bulk material. Our group has recently focused on methods using metal particles dispersed in dense pellets as a means of studying lattice strains by conventional methods.[6,7] The thermal expansion properties of Cu- and Ga-doped Pr_2NiO_4 are shown in Figure 1. If it is assumed that the metal is uniformly dispersed throughout the bulk material during sintering, the different thermal expansion coefficients of the metal and the bulk can be predicted to induce a residual strain that will lead to chemical relaxation. As an example, the dispersion of Au in $Pr_{1.90}Ni_{0.71}Cu_{0.21}Ga_{0.05}O_{4+\delta}$ (PNCG) results in the lattice expansion of Pr_2NiO_4, because the thermal expansion of Au is slightly higher than that of PNCG. As expected, the tensile strain induced by dispersing Au in PNCG resulted in increase in the electronic conductivity and oxygen diffusivity of the material.[6,7] Since this sample preparation method generates bulk pellets, the specimens are readily analysed to assess the details of changes in electrical conductivity, oxygen permeability and oxygen nonstoichiometry. To date, we have primarily studied the dispersion of Au in PNCG. However, in the present study, a new combination consisting of Pt and PNCG was investigated to assess the effects of the resulting mechanically-induced lattice strain on PNCG. Since the thermal expansion coefficient of Pt (8.8×10^{-6} K^{-1}) is less than that of PNCG,[8] it is expected that the dense bulk PNCG will be compressed following the dispersion of Pt particles. The difference in thermal expansion properties between Pt and PNCG is more pronounced compared with that between Au and PNCG, as shown in Figure 1, and thus it was anticipated that the application of Pt could result in a greater change in the bulk conducting properties.

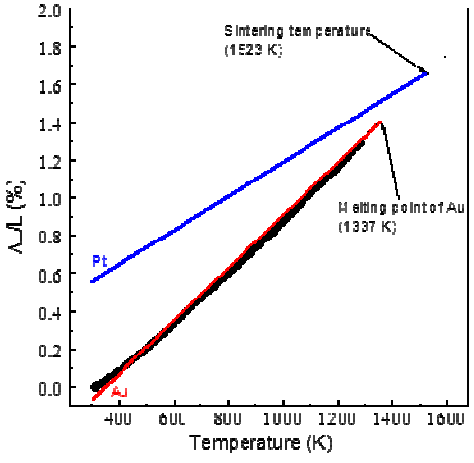

Figure 1 Thermal expansion properties of PNCG, Au and Pt. It is assumed that sintering temperature and melting point of Au are the strain free state of Pt/PNCG and Au/PNCG, respectively.

Experimental

[a] Department of Applied Chemistry, Faculty of Engineering, Kyushu University, Motooka 744, Nishi-ku, Fukuoka Japan, 819-0395
[b] International Institute for Carbon Neutral Energy Research (WPI-I2CNER), Kyushu University, Motooka 744, Nishi-ku, Fukuoka Japan, 819-0395

Dense pellets of x mol% Pt dispersed in PNCG (x = 0, 0.5, 1 and 2) were fabricated by sintering powdered mixtures of Pt and PNCG prepared using the solid state reaction method. $Pr(NO_3)_3{\cdot}6H_2O$ (99.9%, Mitsuwa Chemicals Co., Ltd.), $Ni(CH_3COO)_2{\cdot}4H_2O$ (98%, Wako Pure Chemical Industries, Ltd.), $Cu(NO_3)_2{\cdot}3H_2O$ (99%, Wako Pure Chemical Industries, Ltd.), $Ga(NO_3)_3{\cdot}nH_2O$ (99.99%, Mitsuwa Chemicals Co., Ltd.) and $[Pt(NH_3)_4](NO_3)_2$ (99.995%, Sigma-Aldrich Co. LLC.) were used as starting materials. The details of the pellet preparation method have been reported elsewhere.[6,7,9,10] The densities of the obtained pellets were found to be at least 90% of the theoretical values, which was considered sufficient. It is also noteworthy that all sample pellets exhibited very similar densities, regardless of the proportion of dispersed Pt particles that they contained. The crystal structures of these samples were examined by X-ray diffraction (XRD, Smart Lab, Rigaku) and their morphologies were observed via scanning electron microscopy (SEM, Versa 3D, FEI). Backscattered electrons (BSE) were used to clearly observe Pt particles based on the Z-contrast. The electrical conductivities of the samples were measured in air by a DC 4-probe method at temperatures ranging from ambient to 1173 K. The variations in conductivity with changes in the oxygen partial pressure were also assessed, by introducing various mixtures of O_2 and N_2 to the measurement chamber. The oxygen partial pressures in these mixtures were determined with a Ca-stabilized ZrO_2 oxygen sensor positioned in close proximity to the sample. Seebeck coefficients were measured at temperatures ranging from ambient to 1173 K for estimating changes in the charge carrier concentration and the measurement was performed by using commercial measurement system (R2001i-G, Ozawa Science Co. Ltd.). P_{O2} dependency of Seebeck coefficients were also measured from 10^0 to $10^{-4.5}$ atm. In these measurements, a bar-shape sample was employed together with a Pt electrode and Pt line. A temperature gradient was obtained by cooling one side of the sample via a cold air feed through a quartz tube, while measuring the sample temperature using a Pt-PtRh thermocouple. The oxygen permeability values of specimens were determined so as to confirm the lattice strain effect on the oxide ion conductivity; the details of the measurement conditions have been described elsewhere.[10] The thermal expansion coefficient of a bar-shaped PNCG specimen was determined with a commercially-available test apparatus (TMA8310, Rigaku) in air at temperatures ranging from ambient to 1273 K. X-ray photoelectron spectroscopy (XPS) analyses were performed on polished PNCG and 1 mol% Pt/PNCG specimens using a commercial spectrometer with Al-K_α radiation (Shimadzu, AXIS-165). Before the measurement Au was sputtered on the surface to define the standard binding energy position. The obtained spectra were normalized by compensating the Au 4f binding energy to 84 eV. Oxygen content of Pt dispersed PNCG was measured by redox titration. The sample specimens were annealed at 873 K for 20 h, and then quenched. The obtained samples were dissolved into HCl solution with efficient amount of KI. Precipitated I_2 was titrated using 0.1 M $Na_2S_2O_3$ solution. For the estimation of oxygen nonstoichiometry, the amount of Pt is excluded from the sample weight because it is known that Pt is not dissolved into HCl solution. The electrical conductivity, electronic carrier concentration, and carrier mobility were measured using commercial Hall-effect equipment (Nanometrics, HL5500PC), which can control both temperature and oxygen partial pressure. The measurement was carried out using the Van der Pauw method with polished pellets 0.3 mm thick. The temperature dependence of Hall-effect was measured from 873 K to room temperature in air.

Results and Discussion

The wide-angle XRD patterns and the results of Rietveld refinement for 1 mol% Pt-dispersed PNCG specimens are shown in Fig. 2(a). All diffraction peaks are assigned to those from Pr_2NiO_4 phase with a tetragonal structure, together from a metallic Pt phase. The intensities of the peaks assigned to Pt increased with increasing amounts of dispersed Pt particles, indicating that the Pt did not react with the Pr_2NiO_4-based

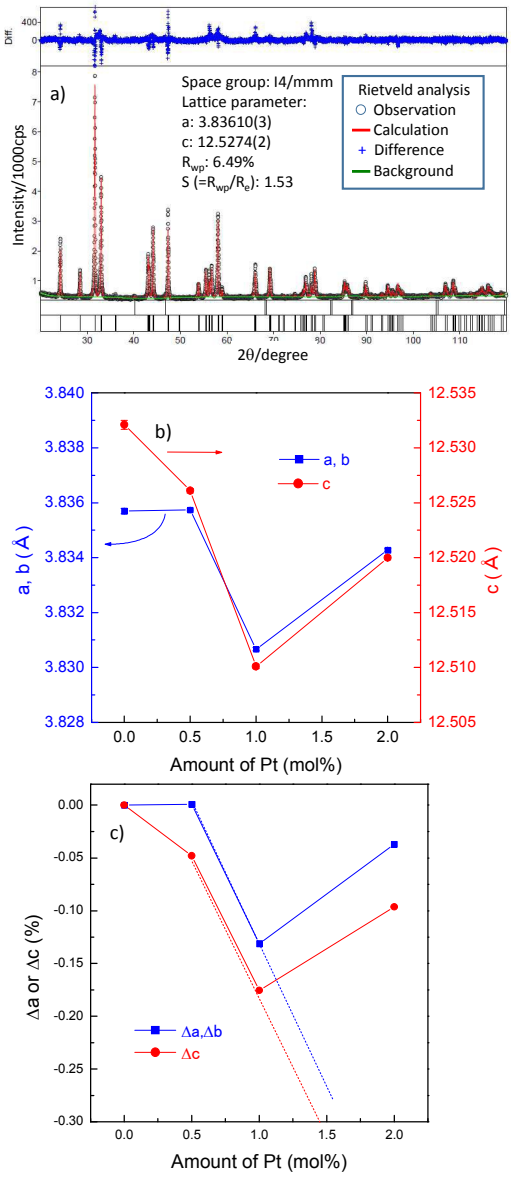

Figure 2 Wide-angle XRD patterns and Rietveld refinement of (a) 1 mol% Pt/PNCG. (b) Variations in lattice parameters in x mol% Pt/PNCG with Pt content. (c) Variations in estimated strains obtained from the lattice constants in (b) with Pt content.

oxides. To allow a quantitative assessment of the strain, the lattice parameters of the various x mol% Pt/PNCG specimens were estimated from the diffraction patterns, and the results are summarized in Fig. 2(b) as a function of the amount of dispersed Pt. Here it is obvious that a, b and c axes were all shortened by the dispersion of Pt. The changes in the unit lattice parameters are also shown in Fig. 2(c) as a function of Pt amount. A compressive strain can be observed along all axes and the amount of strain is varied as a function of the amount of Pt. Because the strain induced by metal dispersion is independent of the crystal orientation due to the completely random dispersion of the Pt particles, the strain observed by XRD over this range may be primarily mechanical. In case of 0.5 mol% Pt , compressive strain was only observed at c axis but not a-axis. The length of c-axis is sensitively changed by the amount of interstitial oxygen. Since 0.5 mol% Pt is small and dispersion of Pt is limited, the introduced compressed strain by 0.5 mol% Pt seems to be small and un-uniform resulting in the shrinkage of c-axis was only observed. The compressive strain generated in the 1 mol% Pt/PNCG specimen was more clearly observed and this was 0.14 %. If we assume that the mechanical strain varies in a linear manner with the amount of dispersed metal, the predicted compressive strain can be extrapolated as shown by the dotted line in Fig. 2(c). However, the observed unit lattice constant of the 2 mol% Pt-loaded PNCG was larger than that of the 1 mol% Pt/PNCG. The reason for this lattice expansion might be related to the chemical strain obtained when introducing interstitial oxygen into the rock-salt block in K_2NiF_4-type structure. K_2NiF_4-type structure is possible to introduce the interstitial oxygen in the rock salt layer, which increase the lattice along c-axis direction. This introduction of interstitial oxygen expanded the c-axis with 2 mol% Pt dispersion. Although it is unexpected that chemically induced strain can be result from mechanical strain, it is at least evident that a mechanical compressive strain was successfully introduced in the PNCG by Pt dispersion.

SEM observations were performed to examine the morphology of the samples, in particular, the Pt state and microstructure of the PNCG around the Pt particles. The resulting BSE images are presented in Fig. 3. The strong contrasts evident in these images are related to the Z-contrast, and the white spots indicate Pt particles. The low magnification image in Fig. 3(a) shows several Pt particles. These are not uniform with regard to size but rather vary in diameter from 1 to 3 μm. Micro-crack or pore structures were evidently formed at the interface between PNCG and Pt in the case of larger particles, which can be explained by the large difference in thermal expansion coefficient between Pt and PNCG. There was no micro-crack formation around the Pt particles smaller than 1 μm, and therefore improved dispersion of the particles is important in terms of effectively inducing mechanical strain. This issue is currently being investigated in more details. A BSE image acquired with higher magnification is shown in Fig. 3(b), from which it can be seen that micro pores were formed at the interface between Pt and PNCG, possibly corresponding to the region of effective compressive strain, since these small pores were only observed at the interfaces. Fig. 3(c) shows X-ray images of the Pt, O and Pr distributions in this sample. Here the bright contrast regions indicate strong Pt signals, and it can be seen that there are no O signals present in these same regions. Therefore, Pt was not oxidized but rather maintained its metallic state after dispersion in the PNCG. Furthermore, Pt signals were not detected in the PNCG regions, indicating that the Pt did not react and also did not diffuse into PNCG. As noted, SEM observations indicated successful dispersion of metallic Pt particles into the PNCG bulk but with the formation of micro pores at the Pt/PNCG interfaces, possibly as the result of chemical reduction due to the oxygen deficiency caused by the compressive strain. One possible mechanism for an oxygen evolution reaction in this material can be presented using Kröger-Vink notation as Eqs. (1) and (2).[11]

$$O_i'' \rightarrow V_i^x + \frac{1}{2}O_2(gas) + 2e' \quad (1)$$

$$O_O^x \rightarrow \frac{1}{2}O_2(gas) + V_O^{\cdot\cdot} + 2e' \quad (2)$$

Both Eqs. (1) and (2) involve the generation of electrons and, since PNCG is a p-type conductor,[9,10,12] these electrons decrease the hole concentration ($h^{\cdot} + e' = X$). To assess this possibility, the electrical conductivities of x mol% Pt/PNCG specimens were measured. It is noted that the difference of particle size were not significant, which seemed not to affect the electrical conductivity.

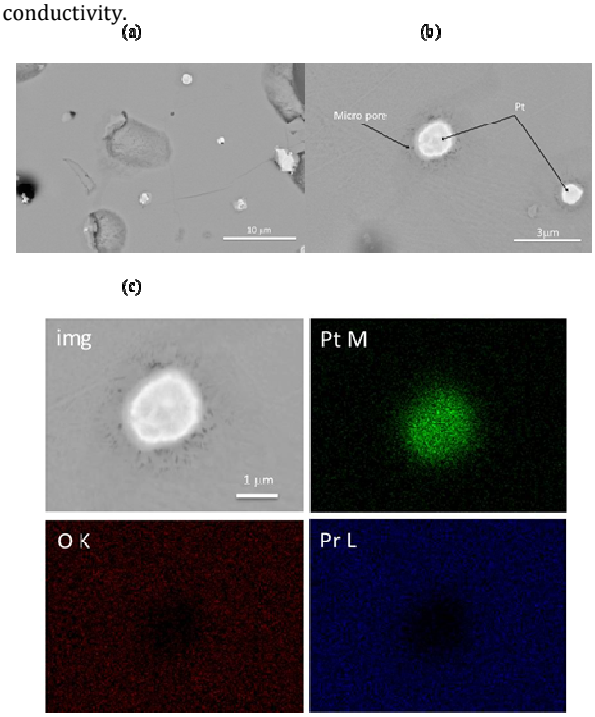

Figure 3 (a) Backscatter electron (BSE) image of a 1 mol% Pt/PNCG. (b) Higher magnification BSE image of regions around Pt particles. (c) X-ray images for Pt, O and Pr in the vicinity of a Pt particle.

Figure 4(a) presents Arrhenius plots of the electrical conductivity values as functions of the amount of dispersed Pt. As expected from Eqs. (1) and (2), the conductivity was decreased. Furthermore, the temperature dependencies of the Seebeck coefficients of PNCG and x mol% Pt/PNCG (x=0.5, 1, 2) are shown in Fig. 4(b). Because the Seebeck coefficient (denoted as S) can be determined from Eq. (3) by assuming constant charge mobility, where e is the electronic charge, k_B is the Boltzmann constant, C is the carrier density, NC is the effective density of states of the valence band (DOS) and A is a transport constant, it is possible to determine changes in carrier concentrations from S.[15]

$$S = \frac{k_B}{e}\left\{ln\left(\frac{N_C}{C}\right) + A\right\} \quad (3)$$

Both Pt-free PNCG and x mol% Pt/PNCG exhibit positive Seebeck coefficients at all test temperatures, indicating that the main carriers in both samples were electron holes. The Seebeck coefficient was increased by the addition of Pt, indicating that the hole concentration was decreased. These results are in good agreement with predictions made based on the hypothesis of micro pore formation via the reactions in Eqs. (1) and (2). Furthermore, the Seebeck coefficients of 2 mol% Pt/PNCG were slightly decreased compared with that of 0.5 and 1 mol% Pt/PNCG. This means hole concentration of 2 mol% Pt/PNCG is higher than that of 0.5 and 1 mol% Pt/PNCG. As a result, electrical conductivity of 2 mol% Pt/PNCG shows lowest conductivity in this series, suggesting the hole mobility decreased at 2 mol% Pt/PNCG. This could be related with the chemical relaxation of compressed strain by Pt. As discussed earlier, the lattice constant of 2 mol% Pt/PNCG increased compared with 1 mol% Pt/PNCG, and which is expected to be due to the introduction of interstitial oxygen. In addition, the hole formation in PNCG has been shown by the reverse reaction given in Eq. (4).[12,14] Therefore, decreased hole concentration corresponded to the decreased amount of interstitial oxygen in the K_2NiF_4 structure. The interstitial oxygen compositions of Pt/PNCG at 873 K were measured by redox titration, and results are summarized in Table.1. As expected, decreased amount of interstitial oxygen in K_2NiF_4 structure was confirmed. Therefore, it can be said that inducing the mechanical compressive strain by Pt dispersion decreased the hole concentration. The oxygen hyper-stoichiometry in 2 mol% Pt/PNCG should be larger than that of 0.5 or 1 mol% Pt/PNCG according to the results of Seebeck coefficient measurements shown in Fig. 4 (b), however, this method does not confirm the deference in oxygen

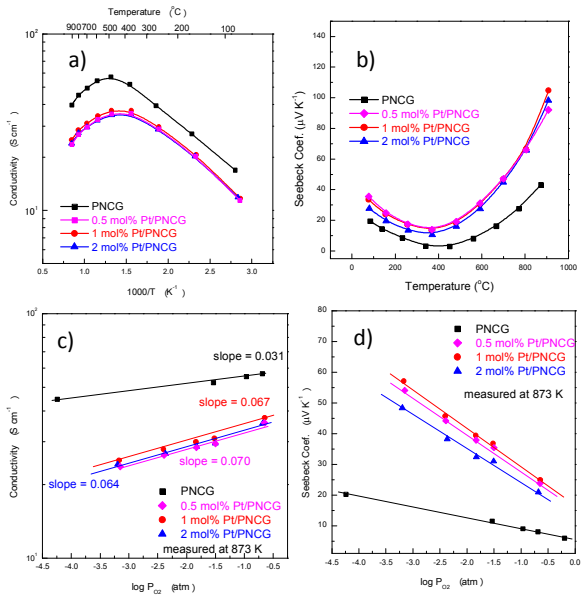

Figure 4 (a) Arrhenius plots of the electrical conductivity of x mol% Pt/PNCG (x = 0, 0.5, 1 and 2). (b) Variations in the Seebeck coefficients of x mol% Pt/PNCG (x = 0, 0.5, 1 and 2) with temperature. (c) Electrical conductivity of x mol% Pt/PNCG (x = 0, 0.5, 1 and 2) as a function of oxygen partial pressure. (d) Seebeck coefficients of x mol% Pt/PNCG (x = 0, 0.5, 1 and 2) as a function of oxygen partial pressure.

composition between 0.5 or 1 mol% Pt/PNCG and 2 mol% Pt/PNCG. According to Eq. (3), the carrier concentration can be expressed by Eq.(4)

$$C \propto \left\{exp\left(\frac{eS}{k_B}\right)\right\}^{-1} \quad (4)$$

In order to confirm the change in hole concentration, the oxygen partial pressure dependence of the conductivity was measured. As shown in Fig. 4(c), it was seen that dispersing Pt increased the P_{O2} dependency of conductivity by 2 times, and this means formation of interstitial oxygen according to Eq. (1) is easier comparing with the sample without Pt dispersion. It is still not clear the reason why the amount of interstitial oxygen is changed by Pt dispersion, however, a change in the hole concentration is evidently associated with the chemically induced strain that is strongly related with the mechanical strain resulting from dispersed Pt. Considering the small amount of Pt, the significant change in conductivity could be related with chemical relaxation of induced mechanical strain. In this point of view, the strain effects in this study are not simple mechanical compressed strain but mechano-chemical strain effects. However, further analyses are required to understand the mechanism of the mechano-chemical strain.

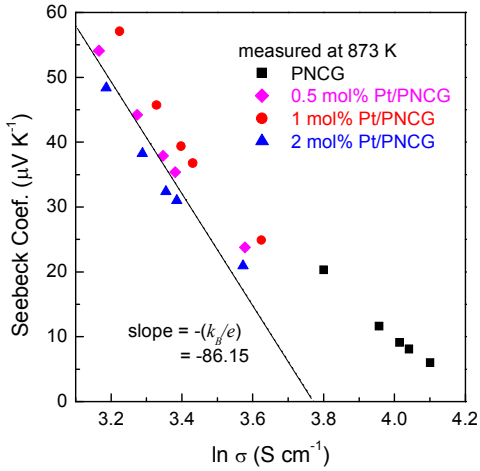

Figure 5 Jonker Plots of P_{O2} dependency of Pt/PNCG at 873 K.

Oxygen composition can be also discussed from Seebeck coefficients. As summarized in Table.1, the ratio of the hole concentration in Pt/PNCG estimated from Seebeck coefficient is almost the same with that from redox titration. Therefore, it is concluded that obtained oxygen nonstoichiometry and Seebeck coefficient agrees each other, and that decrease in electrical conductivity by dispersing Pt is assigned to the decreased hole concentration.

The conductivity and Seebeck coefficient was further analyzed by using Jonker plots and the results are shown in Fig.5. Since Seebeck coefficient can be written as follows by transforming Eq.(3) using electrical conductivity;

$$S = -\frac{k_B}{e}[ln(\sigma) - ln\{N_c e\mu \cdot exp(A)\}] \quad (5)$$

where σ and μ are the electrical conductivity and the electron (or hole) mobility, respectively. According to the equation (5), a plot of S versus ln (σ), called a Jonker plot, will have a slope of $-(k_B/e) = -86.17$ μV/K, with its intercept on

the ln(σ_0) axis. This intercept will be referred to the "DOS-mobility product," and related with the change in carrier density and its mobility. Figure 5 shows Jonker plots for P_{O2} dependency of Pt/PNCG. As shown in Fig.5, slope of Seebeck coefficient and ln(σ) plots at 873 K is close to -86.17 mV/K and so the hole in Pt/PNCG behaves as point defects in both non Pt and Pt dispersed samples. As shown in Fig.5, change in Jonker plots by Pt addition is observed at intercept which represents the number of charge and its mobility in Pt amount from 0.5 to 2 mol%. Since it is assumed that Pt addition may not change significantly the mobility because of the same matrix of PNCG, change in conductivity by dispersion of Pt could be also explained by decrease in hole concentration.

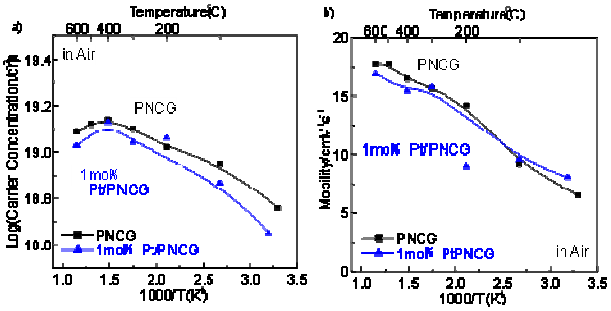

Figure 6 (a) Temperature dependence of hole concentration and mobility of PNCG and 1 mol% PNCG estimated by Hall effect measurement.

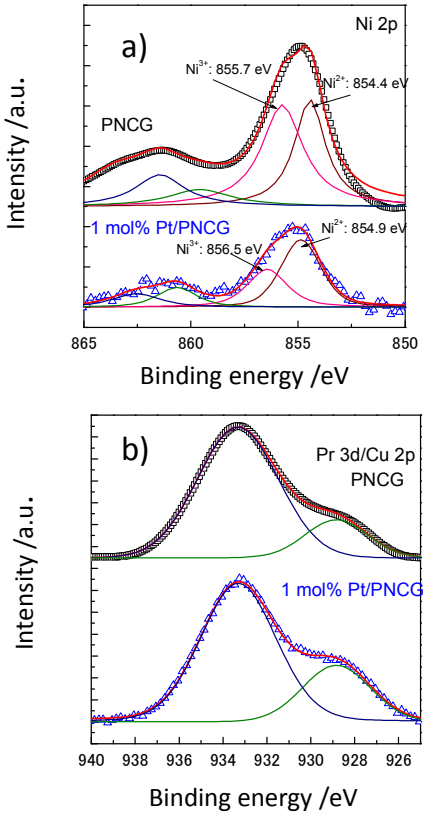

Figure 7: XPS spectra of (a) Ni 2p (b) Pr 3d/Cu 2p in PNCG and 1 mol% Pt/PNCG. The PNCG spectra are reproduced from [Ref. 7].

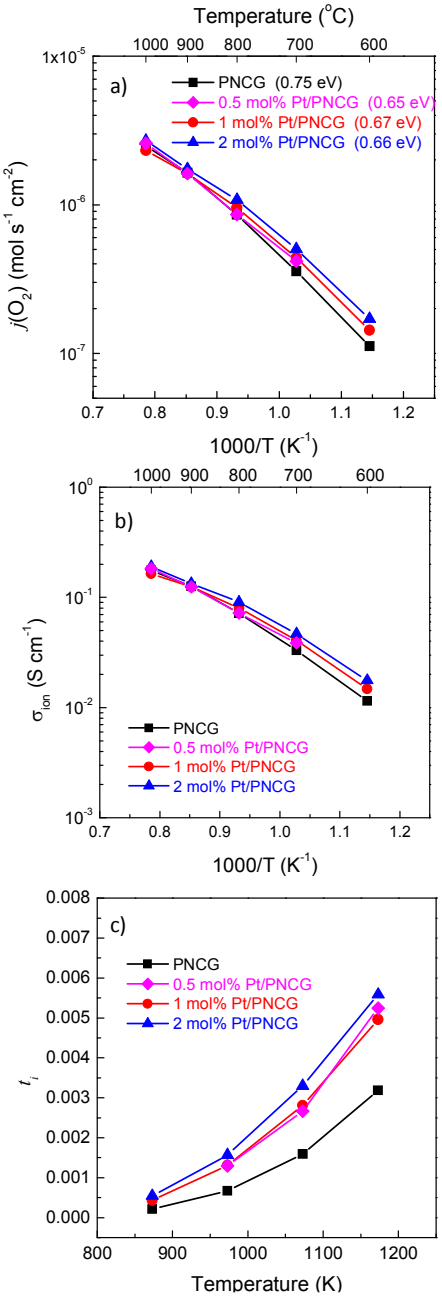

Figure 8: (a) Arrhenius plot of oxygen flux (j_{O2}) as a function of Pt amounts, x (x = 0, 0.5, 1 and 2). (b) Estimated oxide ion conductivity of x mol% Pt/PNCG (x = 0, 0.5, 1 and 2) (c) Transport number of oxide ion in x mol% Pt/PNCG (x = 0, 1 0.5, and 2).

In order to confirm the change in charge carrier concentration, temperature dependence of Hall effect was measured on PNCG and 1 mol% Pt dispersed one in air. This is because the most significant compressed strain effects were observed as shown in Fig.2. Since positive Hall coefficient was observed on PNCG with and without Pt, it is obvious that the hole conduction is dominant in PNCG in air and this is good agreement with P_{O2} dependence of the electrical conductivity (Fig.4.(c)) and Seebeck

coefficient measurement. Figure 6 shows the estimated hole concentration and mobility of the sample with and without Pt dispersion. Obviously, mobility is hardly changed by 1 mol% Pt dispersion (Fig.6(a)), however, hole concentration was decreased by dispersion of 1 mol% Pt as shown in Fig.6 (b). Therefore, Hall effect measurement also suggested that the compressed strain caused by Pt dispersion decreases the hole concentration resulting in decrease in electronic conductivity.

Figure 7(a) shows the Ni 2p XPS spectra of PNCG and 1 mol% Pt/PNCG. In our previous work, the average oxidation number of Ni was shifted to higher values by the addition of Au[7], and so the effects of Pt on the average Ni valence number were also assessed.[7,16–19] For estimating Ni^{3+}, peak deconvolution was performed as shown in Fig. 7(a). The peaks at 854 and at 857 eV (both indicated by dashed lines) were assigned to Ni^{2+} and Ni^{3+}, respectively, [16-19] and the Ni^{2+} to Ni^{3+} ratio was estimated from the peak areas. The estimated volume fractions of Ni^{3+} species were 56 and 38 % in the PNCG and 1 mol% Pt/PNCG, respectively. As discussed above, the mechanically compressed 1 mol% Pt/PNCG exhibited decreased conductivity related to its decreased hole concentration. This is because Ni^{3+} is considered as hole trapped state of Ni^{2+}. The lower amount of Ni^{3+} in this specimen is therefore in good agreement with the electronic conductivity and Seebeck coefficient measurements. The ionic radii of Ni^{2+} and Ni^{3+} are 0.69 and 0.56 Å, respectively. Even though the lattice parameters of 1 mol% Pt/PNCG were decreased compared with those of the original PNCG, the amount of Ni^{2+} in the PNCG, which has a larger ionic radius than Ni^{3+}, was larger. This result indicates that the Ni sites in the PNCG began to expand chemically as they were repelled by the mechanical compression strain, and this chemical expansion was dominant after the level of dispersed Pt reached 2 mol%, as is evident from Figure 2(d). Figure 7(b) shows the overlapped Pr 3d and Cu 2p peaks. Because these peaks appear at exactly the same binding energy position, it is impossible to observe the chemical states of Pr and Cu separately. However, an increased peak area at 929.5 eV was observed in the case of 1 mol% Pt/PNCG. This change demonstrates that, as expected, in addition to the Ni, the Pr and/or Cu are also transitioned to a reduced state by the Pt dispersion, and that different cation oxidation states were achieved in the Pr_2NiO_4 by the simple addition of Pt.

Oxygen permeation rates was measured at 0.5, 1 and 2mol% Pt dispersion, as shown in Figure 8 (a), for confirming the effect of the mechano-chemically induced compressive strain on ion transport in these materials. Oxygen permeation flux (denoted as j_{O2}) was changed by Pt dispersion, particularly, at lower temperature. The activation energy for the oxygen permeation rate was decreased from 0.75 to 0.66 eV by compressive strain. The oxygen permeability can be expressed by Eq. (6) when bulk diffusion is limited the permeation;

$$j_{O_2} = \frac{RT\sigma_e\sigma_i}{16F^2(\sigma_e+\sigma_i)d} ln\frac{p_{high}}{p_{low}} \approx \frac{RT\sigma_i}{16F^2 d} ln\frac{p_{high}}{p_{low}} \quad (\sigma_e \gg \sigma_i), \qquad (6)$$

where R is the gas constant, T is the temperature, F is the Faraday constant, σ_e is the electronic conductivity, σ_i is the ionic conductivity, d is the thickness of the specimen and p_{high} and p_{low} are the oxygen partial pressures at high and low concentration, respectively. If the σ_e value is sufficiently higher than the ionic conductivity, the oxygen flux can be approximated as shown in Eq. (6), that is, the oxygen flux is proportional to the oxide ionic conductivity. Additionally, the oxide ionic conductivity can be calculated as the product of the oxide ionic carrier concentration and mobility. Considering the decreased hole concentration and the interstitial oxygen amount by dispersing Pt metals, increase in oxygen flux is not associated with increased ionic carrier concentration, but mobility. Figure 8(b) shows the oxide ionic conductivity estimated from Eq.(6) as a function of 1/T. High oxide ionic conductivity was estimated in PNCG with or without Pt dispersion but ionic conductivity was increased by dispersion of Pt. [12] As a result, the estimated ionic transport number in Pt/PNCG is smaller than 1 % as shown in Figure 6(c). Therefore, Eq.(6) can be applied to estimate oxide ion conductivity. Since carrier concentration and mobility cannot be separated by the oxygen permeation rate, further detail study is required to elucidate the changes in ion transport property. For the estimation of oxygen of mobility, Nernst-Einstein relationship which is shown as Eq.(7) is used, where D_i is interstitial oxygen diffusivity, c_i is interstitial oxide ion concentration shown in Table.1.

$$\sigma_i = \frac{(2e)^2 c_i}{k_B T} D_i \quad (7)$$

Obtained D_i of x mol% Pt/PNCG (x = 0, 1, 2) are shown in Table.1. It is obvious that 5-6 times more significant diffusivity than that of PNCG is obtained. Therefore, it is obvious that the mechano-chemical strain caused by Pt dispersion changes the oxygen nonstoichiometry of PNCG, resulting in variations in both the oxide ionic carrier concentration and mobility. Moreover, such changes also greatly affect the electrical conductivity of the material.

Table 1 Oxygen content in PNCG at 873 K measured by redox titration and the ratio of hole concentration and estimated chemical diffusion coefficients (D_{Chem}) by the oxygen permeation measurement in Pt/PNCG to Pt-free PNCG .

Sample	Oxygen content 4+δ (at 873 K)	$[O_i'']$ (cm^{-3}) (at 873 K)	$\{\exp(eS/k_B)\}^{-1}$ /$\{\exp(eS(PNCG)/k_B)\}^{-1}$	D_i ($cm^2 s^{-1}$) (at 873 K)
PNCG	4.092 [7]	1.0×10^{21}	1	1.4×10^{-6}
1 mol% Pt/PNCG	4.022±0.009	2.4×10^{20}	0.27	6.9×10^{-6}
2 mol% Pt/PNCG	4.023±0.006	2.5×10^{20}	0.27	8.3×10^{-6}

Conclusion

Effects of Pt dispersion (0.5, 1, and 2 mol%) in Cu- and Ga-substituted Pr_2NiO_4 on electrical conductivity and oxide ion transport properties as the result of mechanically and/or chemically induced compressed strain were studied. Pt dispersion was found to induce a mechanically compressive strain due to the small thermal expansion coefficients of the metal and the bulk material. This study suggests the possibility that this mechanical strain induces an associated chemical strain due to changes in the valence number of Pr, Ni and Cu, as well as variations in the quantity of oxygen defects (oxygen vacancies or interstitial oxygen). These chemo-mechanical strains have a significant effect on the oxide ion and charge transfer properties of the material. At present, the reason why compressed strain is not significantly observed at higher amount of Pt is not clear,

however, considering the large mismatch in thermal expansion coefficient between PNCG and Pt and high melting temperature of Pt, microcrack and/or micropore at interface between PNCG and Pt are anticipated and also aggregation of Pt is considered. However, by changing the hole and interstitial oxygen concentrations, the dispersion of a small amount of metallic Pt (or Au)[6,7] evidently modifies the oxygen nonstoichiometry in mixed conductors such as Pr_2NiO_4 and the attendant chemically-induced strain appears to affect the mass transport of oxide ions. Compared to the use of nano-thickness films, metal dispersion in bulk materials should be extremely useful in practical applications such as oxygen separation membranes with improved permeation rates. The use of finer metal particles may generate improved dispersion states and thus introduce the strain more efficiently, which could lead to greatly increased oxygen permeability while preventing microcrack or micropore formation. This concept is now under investigation and the results will be reported in the future.

Acknowledgements

This work was supported in part by a Grant-in-Aid for Scientific Research (S) (no. 24226016) and by the Advanced Low Carbon Technology Research and Development Program (ALCA).

References

1. J. Garcia-Barriocanal, A. Rivera-Calzada, M. varela, Z. Sefrioui, E. Iborra, C. Leon, S. J. Pennycook and J. Santamaria, *Science*, **321**, 676 (2008).
2. A. Kushima and B. Yildiz, *J. Mater. Chem*., **20**, 4809 (2010**)**.
3. C. Korte, A. Peters, J. Janek, D. Hesse and N. Zakharov, *Phys. Chem. Chem. Phys.*, **10**, 4623 (2008).
4. M. Burriel, G. Garcia, J. Santiso, J. A. Kilner, R. J. Chater and S. J. Skinner, *J. Mater. Chem.*, **18**, 416 (2008).
5. D. Pergolesi, E. Fabbri, S. N. Cook, V. Roddatis, E. Traversa and J. A. Kilner, *ACSNANO*, **6**(12), 10524 (2012).
6. J. Hyodo, K. Tominaga, Y.-W. Ju, S. Ida and T. Ishihara, *ECS Trans.*, **61**(1), 123 (2014).
7. J. Hyodo, K. Tominaga, J.-E. Hong, S. Ida, T. Ishihara, *J. Phys. Chem. C.,* **119**, 5, (2015).
8. R. E. Edsinger, M. L. Reilly, and J. F. Schooley, *J. Res. Nat. Bur. Stand.*, **91**(6), 333 (1986).
9. T. Sekino and K. Niihara, *J.Mater. Sci*., **32**, 3943, (1997).
10. J. Selsing, *J. Am. Ceram. Soc.*, **44**, 419, (1961).
11. T. Ishihara, K. Nakashima, S. Okada, M. Enoki and H. Matsumoto, *Solid State Ionics*, **179**, 1367 (2008).
12. T. Ishihara, N. Sirikanda, K. Nakashima, S. Miyoshi and H. Matsumoto, *J. Electrochem. Soc.*, **157**(1), B141 (2010).
13. F. A. Kröger and H. J.Vink, *Solid State Physics – Advances in Research and Applications,* Academic Press, New York (1957).
14. J. Hyodo, K. Tominaga, Y.-W. Ju, S. Ida and T. Ishihara, *Solid State Ionics*, **256**, 5 (2014).
15. Y. Kinemuchi, C. Ito, H. Kaga, *J. Mater. Res.*, **22**(7), 1942 (2007).
16. M. W. Roberts and R. St. C. Smart, *J. Chem. Soc. Faraday I*, **80**, 2957 (1984).
17. A. F. Carley, S. D. Jackson, J. N. O'Shea and M. W. Roberts, *Surf. Sci.*, **440**, L868 (1999).
18. L. M. Moroney, R. St. C. Smart and M. W. Roberts, *J. Chem. Soc. Faraday Trans. I*, **79**, 1769 (1983).
19. A. P. Grosvenor, M. C. Biesinger, R. St. C. Smart and N. S. McIntyre, *Surf. Sci.*, **600**, 1771 (2006).

Graphical Abstract

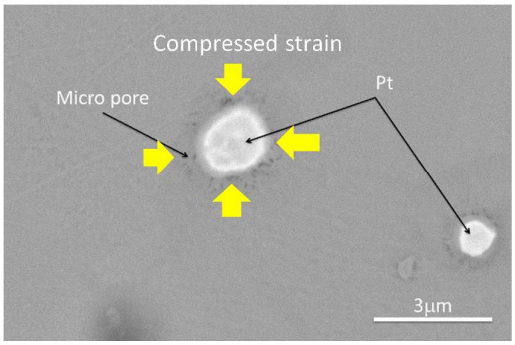

Pt dispersion in Pr_2NiO_4 base oxide formed compressed strain and electrical conductivity decreases, however, oxide ion conductivity increases by the compressed strain due to the decreased hole and the increased interstitial oxygen concentration.